Heart Fail Rev (2017) 22:501–511
DOI 10.1007/s10741-017-9620-9

PET imaging in heart failure: the role of new tracers

Antti Saraste[1,2] · **Juhani Knuuti**[1]

Published online: 5 May 2017

Abstract Positron emission tomography (PET) myocardial perfusion imaging is being increasingly used for the detection of coronary artery disease. In the presence of significant left ventricle dysfunction, the assessment of myocardial ischemia and viability by PET plays a role in the identification of patients who may benefit from revascularization. In addition to these, new PET tracers may play a role in the assessment of underlying pathophysiology and therapeutic options in heart failure. Studies have shown the ability of sympathetic innervation imaging to assess the risk of cardiac death, arrhythmia, and disease progression. New tracers have been tested for the assessment of angiogenesis and other mechanisms involved in myocardial repair after infarction. Furthermore, new tracers may play a role in detection of inflammatory cardiomyopathies, especially cardiac sarcoidosis, which is a diagnostic challenge for current methods. In addition to the assessment of prognosis and etiology, the value of new PET tracers will depend on their ability to guide selection of therapies and incorporation into clinical management algorithms in heart failure. This review describes recent advances in applications of cardiac PET in heart failure with emphasis on potential roles of new tracers.

✉ Antti Saraste
antti.saraste@utu.fi

[1] Turku PET Centre, Turku University Hospital and University of Turku, Kiinamyllynkatu 4-8, 20520 Turku, Finland

[2] Heart Center, Turku University Hospital, Hämeentie 11, 20520 Turku, Finland

Keywords Heart failure · Fibrosis · Angiogenesis · Viability · Perfusion · PET

Introduction

Cardiac imaging is essential for the diagnosis of heart failure (demonstration of cardiac dysfunction and underlying structural heart disease), to determine its mechanisms (heart failure with reduced or preserved systolic function) and studying etiology (presence of myocardial infarction or ischemic heart disease, valvular heart disease, or cardiomyopathy) [1]. Imaging also plays an important role in determining prognosis and tailoring heart failure therapy, including revascularization, medical therapies, and device therapy with cardiac resynchronization pacemaker and/or implantable cardiac defibrillator to improve symptoms and prognosis [1, 2]. It has been increasingly recognized that detailed evaluation of underlying pathophysiology is essential for the successful development and application of new therapies for heart failure [3].

Positron emission tomography (PET) myocardial perfusion imaging is frequently used for detection of ischemic etiology of heart failure and evaluation of the extent of viable ischemic myocardium before revascularization. Improvement in PET imaging technology has led to evolution of PET imaging beyond the isolated assessment of myocardial perfusion, toward characterization of molecular processes at the cardiac tissue level. Molecular imaging aims at visualization of specific molecular targets that precede or underlie changes in morphology, physiology, and function. Nuclear imaging provides very high detection sensitivity for molecular-targeted imaging of biological processes involved in heart failure, such as myocardial metabolism, innervation, inflammation, and extracellular matrix remodeling. This review describes advances in

application of new PET tracers in heart failure with discussion on their potential roles.

Technical aspects of PET

PET imaging represents an advanced technique to map radiotracer concentration and kinetics in the myocardium [4, 5]. With the currently applied PET scanners and post-processing algorithms, images can be reconstructed with a spatial resolution of 4–7 mm. Outstanding sensitivity allows for identification of radiotracer at nano- or picomolar concentrations. With the use of validated photon attenuation and scatter correction algorithms, PET imaging can be used to quantify the absolute amount of nuclear tracer within the myocardium. Relatively high temporal resolution of PET allows the development of dynamic images, which can be used to assess tracer kinetics.

Several recent developments have contributed to application cardiac PET for assessment of heart failure [4, 5]. The availability of PET systems and cyclotrons needed to produce tracers has markedly increased due to its increasing use in oncology. New radiotracers have been introduced, which have the potential to improve availability of cardiac PET and extend the current possibilities for molecular imaging [6–8] (Table 1). At the same time, several technical advances have been introduced that improved detection sensitivity and image resolution that allow detection of weak signals coming from molecular-targeted tracers. Development of detector technology has resulted in growth in count rate performance of scanners and new reconstruction algorithms have been introduced that decrease noise in the images [4]. Furthermore, addition of cardiac and respiratory gating of PET images has potential to further increase in detection sensitivity in cardiac PET [9]. PET scanners are increasingly integrated with either computed tomography (CT) or cardiac magnetic resonance (MR) systems into PET-CT or PET-MR hybrid imaging devices, which facilitate the localization of a molecular signal, by fusion with high-resolution morphologic images [10].

Myocardial perfusion imaging

Ischemic cardiomyopathy is the most common cause of heart failure. From 24 multicenter heart failure trials, including 443,568 heart failure patients, 62% of patients had an ischemic etiology [11]. Myocardial perfusion imaging represents a well-established imaging modality for the evaluation of location, extent, severity, and reversibility of myocardial perfusion defects in patients with known or suspected coronary artery disease (CAD), contributing to the detection of ischemic etiology of heart failure [12, 13]. PET myocardial perfusion imaging provides good image quality, certainty of interpretation, and diagnostic accuracy for the detection of CAD. In two meta-analyses of diagnostic studies including 1394 to 1692 patients, pooled sensitivity of PET myocardial perfusion imaging varied from 84 to 90% and specificity from 84 to 88% in the detection of obstructive CAD defined as ≥50 or ≥70% stenosis on invasive coronary angiography [12, 13]. Similar to SPECT, the extent and severity of PET perfusion defects have strong incremental prognostic value beyond traditional cardiovascular risk factors [14].

In addition to the assessment of relative distribution of perfusion, PET with radiotracer kinetic modeling can be used to quantify myocardial blood flow (MBF) in absolute terms (mL/g/min) at rest and during vasodilator stress that allows the computation of coronary flow reserve (CFR). Quantification of regional MBF and CFR by PET may identify microvascular dysfunction, better characterize the extent and severity of CAD burden in multi-vessel disease, and detect balanced decreases of MBF in all major coronary artery vascular territories [15–17]. Furthermore, several studies have demonstrated that reduced CFR is a powerful predictor of increased risk

Table 1 New positron emission tomography tracers and their applications in heart failure

Application	Tracer	Target	Phase	References
Myocardial perfusion	^{18}F-flurpiridaz	Mitochondrial complex 1	Phase II study	[6, 25–31]
Myocardial infarction	^{18}F-Fluciclatide, ^{18}F-galacto-RGD, ^{68}Ga-NODAGA-RGD, ^{68}Ga-PRGD2, ^{68}Ga-DOTA-RGD, ^{68}Ga-NOTA-RGD	Integrin $\alpha_v\beta_3$	Experimental models of MI, patients with acute myocardial infarction or chronic total coronary occlusion	[7, 47–57]
	^{68}Ga-Pentixafor	CXCR4 chemokine receptor	Experimental models of MI, patients with acute myocardial infarction	[60–62]
	^{11}C-KR31173	Angiotensin receptor 1	Experimental models of MI, healthy individuals	[64]
Sympathetic innervation	^{18}F-LMI1195	Sympathetic neuronal catecholamine storage	Phase 1 clinical study and experimental models	[8, 70–72]
Inflammatory cardiomyopathy	^{68}Ga-DOTANOC, ^{68}Ga-DOTATOC	Somatostatin receptors	Patients with cardiac sarcoidosis	[76, 81]

of future cardiac events and it is incremental to the presence of regional perfusion defects or angiographic stenosis [18–21]. In heart failure, it has been shown that global CFR is frequently impaired in cardiomyopathic heart as a consequence of microvascular dysfunction in the absence of epicardial CAD [22, 23]. Outcome studies have supported microvascular dysfunction as an independent contributing factor to the symptoms and progression of heart failure and reduced CFR was a predictor of adverse cardiac events in patients with both ischemic cardiomyopathy [23] and idiopathic dilated cardiomyopathy [22, 23]. However, it remains to be seen whether and how quantitative measurements of CFR can direct therapy in patients with heart failure.

The main limitation of PET perfusion imaging is that perfusion tracers that are currently in clinical use have very short radioactive half-lives. This limits their availability, because an on-site cyclotron or a generator, which requires relatively high volume of patients to be cost-effective, is required. Furthermore, short half-lives limits their applicability for exercise stress. In contrast, pharmacologic stress with simultaneous imaging is used. Currently, a generator produced ^{82}Rubidium (^{82}Rb) is the most commonly used perfusion tracer. In addition to ^{82}Rb, ^{15}O water ($H_2{}^{15}O$) and ^{13}N ammonia ($^{13}NH_3$) are used in clinical myocardial perfusion PET. Detailed description of specific characteristics of these tracers can be found elsewhere [24].

New ^{18}F-labeled perfusion tracers

To overcome problems related to short radioactive half-life, perfusion tracers labeled with ^{18}F have been studied [24]. Perfusion tracers labeled with ^{18}F have longer half-life (110 min) than ^{82}Rb (76 s), $H_2{}^{15}O$ (123 s) or $^{13}NH_3$ (10 min) and therefore, can be distributed to centers that do not have an on-site cyclotron and potentially can be used with exercise. Of the ^{18}F-based PET perfusion radiotracers, ^{18}F-Flurpiridaz (formerly BMS-747158) that was introduced in 2007 is the most thoroughly studied in animal models and is currently undergoing clinical evaluation in phase III studies [6, 24–27].

^{18}F-Flurpiridaz is derived from pyridazinone and binds avidly to mitochondrial complex-1 [6, 26]. Preclinical experience with ^{18}F-Flurpiridaz demonstrated high and stable myocardial uptake that together with low positron range results in good image quality, defect resolution, and accurate delineation of myocardial infarct size [6, 25–27]. A clinical study did not revealed safety concerns regarding the tracer and the results of dosimetry indicate that the radiation exposure of ^{18}F-flurpiridaz injection (approximately 6 mSv) is lower than that of SPECT imaging [28]. In a phase II clinical trial, diagnostic performance of ^{18}F-Flurpiridaz was compared with that of SPECT MPI for the detection of CAD defined as ≥50% stenosis in 143 patients [29]. Image quality and defect resolution were good (Fig. 1). Compared with ^{99m}Tc SPECT, ^{18}F-flurpiridaz PET was associated with higher diagnostic certainty of interpretation (defined as percentage of cases with definitively normal or abnormal interpretation) and sensitivity (61.5 vs. 78.8%, $p = 0.02$) [25]. Additional benefit of ^{18}F-flurpiridaz is that a rest-treadmill exercise protocol was shown to be feasible [28] and has been applied in the phase II and III clinical studies. Myocardial extraction fraction of ^{18}F-flurpiridaz is high (94%) and proportional to myocardial blood that makes ^{18}F-flurpiridaz a good candidate for absolute quantification of MBF [25]. An experimental study showed good agreement between MBF measures obtained with ^{18}F-flurpiridaz and microspheres over a wide range of regional MBF values (0.1–3.0 mL/min/g) in a pig model [30]. More recently, MBF values have been obtained in humans that were at similar level to the commonly accepted values obtained by other methods [31]. Thus, studies with ^{18}F-flurpiridaz have shown encouraging results for implementation of this tracer in clinical PET myocardial perfusion imaging.

Assessment of viability and metabolism

Assessment of residual myocardial glucose uptake with ^{18}F-fluorodeoxyglucose (^{18}F-FDG) PET can be used to detect ischemic myocardium that is dysfunctional, but viable and has potential for recovery of contractile function after revascularization [2]. Viable myocardium shows preserved ^{18}F-FDG uptake, whereas markedly reduced or absent uptake indicates scar formation. A preserved or increased uptake of ^{18}F-FDG in the presence of reduced myocardial perfusion, known as flow-metabolism mismatch, is the most commonly used marker of hibernating myocardium that is capable of functional recovery after revascularization. ^{18}F-FDG PET is the most sensitive technique to detect viability and it predicts functional recovery upon revascularization. A pooled analysis of 24 studies in 756 patients demonstrated a weighed mean sensitivity and specificity of 92 and 63%, respectively, for regional functional recovery, with positive predictive value of 74% and negative predictive value of 87% [32]. Retrospective studies have also indicated lower annualized mortality rates of those with viable myocardium who underwent revascularization (4%) versus those with viability who did not undergo revascularization (17%) [33].

The value of ^{18}F-FDG PET in guiding decisions on revascularization was studied in a randomized trial that assigned 430 heart failure patients with an ejection fraction below 35% to either management assisted by ^{18}F-FDG PET imaging or standard care [34]. The study overall showed only a nonsignificant trend toward reduction in cardiac events for ^{18}F-FDG PET-assisted management versus standard care. However, the study observed long-lasting survival benefits for ^{18}F-FDG

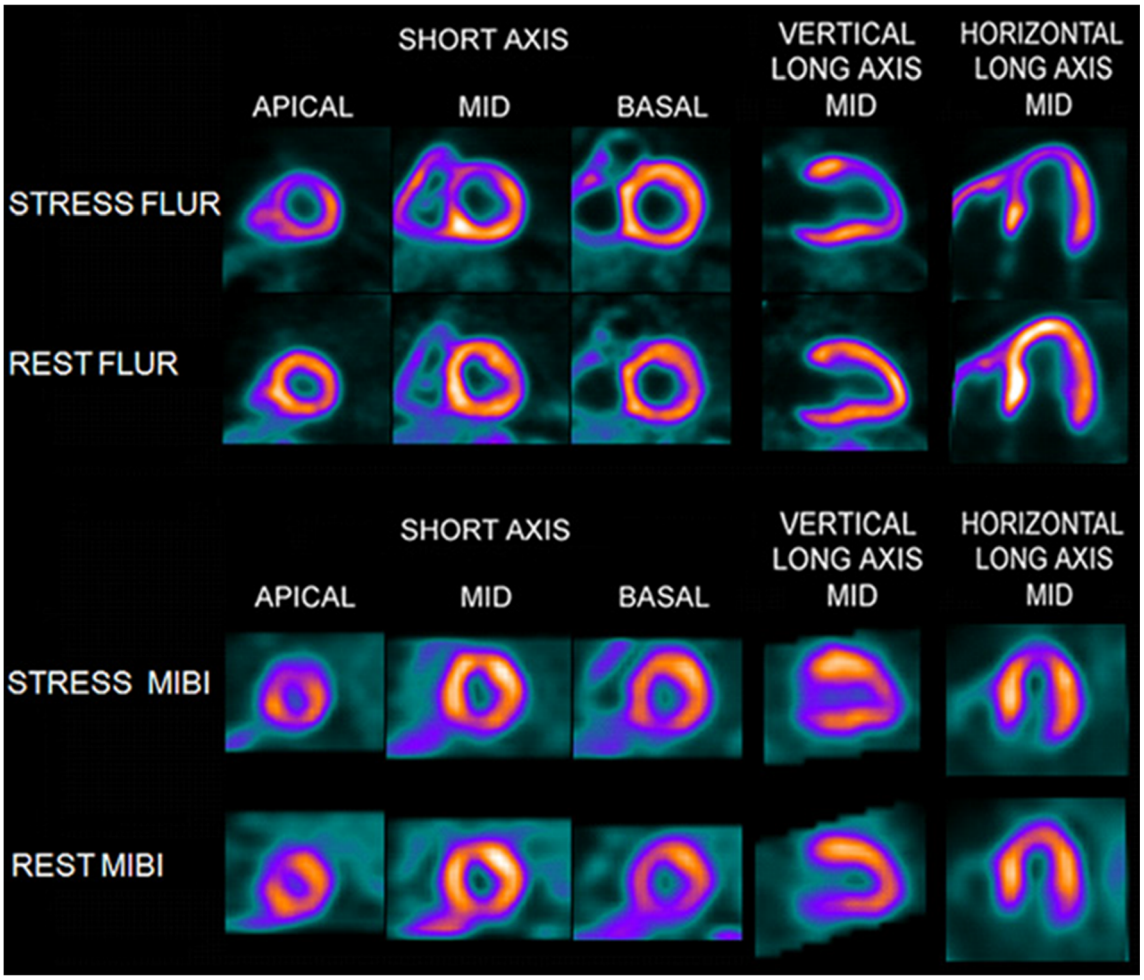

Fig. 1 Myocardial perfusion images obtained with ^{18}F-Flurpiridaz (FLUR) PET (*top*) and Tc-^{99}m sestamibi (MIBI) SPECT (*bottom*). The ^{18}F-Flurpiridaz images show a severe reversible perfusion defect throughout the territory of the occluded proximal left anterior descending coronary artery. The results of the phase II study demonstrated superior image quality, larger defect size, and better diagnostic certainty with ^{18}F-Flurpiridaz PET than SPECT. Image reproduced with permission from ref. 29

PET-assisted management in the subgroup of patients whose treatment adhered to the recommendations by imaging [34, 35]. In a subsequent sub study of the PARR-2 data showed that the outcome benefit was related to the amount of hibernating myocardium seen [36]. Similarly, an observational study evaluating survival benefit from revascularization according to the extent of ischemic, scarred and viable myocardium found a significant interaction with the extent of hibernating myocardium, with a cutoff of >10% indicating survival benefit from revascularization [37].

The role of myocardial viability testing in clinical practice remains controversial [2, 34, 38]. Therapeutic decision-making is often difficult in patients with advanced CAD and severe left ventricular dysfunction due to high procedure-related risks. Therefore, there remains a role for viability imaging, but it is best utilized as an adjunct to decision making for complex patients (i.e., previous revascularization, multiple comorbidities) where both the risks and potential benefits of revascularization are the highest [2]. Viability testing among comprehensive evaluation of heart failure patients might help predict the response to revascularization in selected patients with CAD and left ventricle dysfunction and be a marker of prognosis. Current guidelines recommend the myocardial revascularization should be considered in patients with chronic ischemic heart failure with ejection fraction ≤35% in the presence of viable myocardium [1].

In addition to ^{18}F-FDG, there are other tracers for the assessment of myocardial metabolism that have been used for evaluation of many medical and device therapies on metabolism of the failing heart [39, 40]. ^{11}C-labeled acetate (^{11}C-Acetate) allows robust non-invasive measurement of myocardial oxygen consumption in the left and right ventricles [39]. This provides the means to estimate the oxygen cost of contractility, the efficiency of myocardial forward work. The finding of decreased efficiency of myocardial forward work is a consistent and early finding in heart failure caused by different

etiologies and that can be improved by therapy. ^{18}F-fluoro-6-thia-heptadecanoicacid is a fatty acid analogue, the uptake of which reflects myocardial fatty acid utilization [40], whereas compounds such as ^{11}C-palmitate reflect the flux of fatty acid metabolism through the cell including lipid pool storage, betaoxidation, and tricarboxylicacidcycle flux.

New tracers for myocardial infarction and remodeling

Repair following myocardial infarction is triggered by a complex interaction of neurohormonal activation and upregulation of local paracrine signaling mechanisms that initiate the restoration of capillary network through angiogenesis and extracellular matrix remodeling through macrophage accumulation and fibroblast activation [41–43]. The interplay of angiogenesis, inflammation, and fibrosis determines the restoration of myocardial integrity and eventually contributes to the degree of global remodeling and dysfunction of the left ventricle. New PET tracers targeting the molecular mechanisms underlying repair of myocardial injury have been studied as a potential markers of functional outcome after an acute myocardial infarction. Molecular imaging of the biological processes involved in myocardial remodeling can provide new biomarkers for early detection, evaluation of therapy response, and risk stratification of heart failure.

The $\alpha_v\beta_3$ integrin is a potential target for imaging angiogenesis and repair of myocardial injury. The $\alpha_v\beta_3$ integrin is a transmembrane cell surface receptor that facilitates interaction of cells with the ECM. Expression of $\alpha_v\beta_3$ is an essential mediator of angiogenesis and its expression is markedly upregulated during angiogenesis in the myocardium after infarction [44, 45]. In addition to the endothelium, it is expressed by both activated cardiac myofibroblasts and macrophages after myocardial infarction [45, 46]. Molecular imaging of $\alpha_v\beta_3$ is based on tracers that contain the RGD peptide subunit (the arginine-glycine-aspartate motif) that binds to activated $\alpha_v\beta_3$ integrin. Several PET tracers targeting $\alpha_v\beta_3$ integrin have been evaluated in experimental models of myocardial infarction [44, 46–53], some of them also tested in humans [7, 54–57]. In experimental and human studies of acute myocardial infarction, RGD-based radiotracers accumulate at the site of infarction as early as 3 days, peaking at 1–3 weeks after myocardial infarction and correlating with angiogenesis, infarct scar formation, and adverse remodeling (Fig. 2). A recent study evaluated prospectively $\alpha_v\beta_3$ integrin expression with ^{18}F-Fluciclatide PET in 21 patients with recent myocardial infarction or chronic total coronary occlusion [7]. ^{18}F-Fluciclatide uptake was increased at the site of acute infarction and the degree of uptake was associated with the probability of functional recovery. Imaging of $\alpha_v\beta_3$ integrin may be a potential biomarker to assess functional outcome of infarcted tissue after myocardial infarction and the effects of therapies aimed at accelerating repair after myocardial infarction, such as angiogenic gene therapy [3].

Inflammatory response after myocardial infarction is another target of interest after myocardial infarction. Inflammatory cell imaging has been tested indirectly with metabolic markers ^{18}F-FDG [58] and ^{11}C-methionine [59] to predict functional recovery after myocardial infarction. Recent studies have used a new ^{68}gallium (68Ga)-labeled PET tracer pentixafor that binds to CXCR4 chemokine receptor [60–62]. Paired CXCR4 and its ligand, SDF-1, regulate the migration of hematopoietic stem cells, as well as neutrophils and monocytes from bone marrow and spleen. In experimental and human myocardial infarction, pentixafor uptake was seen in the infarcted region early after the event, was blocked effectively by a CXCR4 inhibitor, and was substantially reduced by neurohumoral antagonists [60]. Pentixafor uptake showed high interindividual variability in patients [61], which may have implications for the response to CXCR4 or other inflammation-targeted therapy, and for subsequent ventricular remodeling.

Myocardial fibrosis is a common feature of left ventricle remodeling after myocardial infarction. Cardiac magnetic resonance (CMR) can provide quantitative measures of myocardial fibrosis, but PET approaches have been assessed to more specifically assess molecular mechanisms underlying fibrosis formation, such as matrix metalloproteinases and neurohormonal activation [42, 63, 64]. The activation of the renin-angiontensin-aldosterone system plays a role in activation of myofibroblasts and is an important mediator of myocardial fibrosis. Molecular imaging approaches targeting angiotensin receptors to measure angiotensin receptor activation have been studied extensively [42]. ^{11}C-KR31173 is a specific and metabolically stable tracer for angiotensin receptor 1 [64]. The feasibility of in vivo imaging myocardial angiotensin receptor 1 with the use of ^{11}C-KR31173 was shown in a pig model of chronic myocardial infarction and the radiotracer was well-tolerated also in humans [64]. Although clinical applications of new tracers for imaging myocardial infarction remain to be determined, studies have shown that molecular imaging of new targets can clarify pathogenesis of heart failure and be potentially useful to study effects of therapies.

New tracers for cardiac sympathetic innervation

Cardiac sympathetic imaging provides a non-invasive approach to risk-stratify patients with heart failure and at risk of sudden cardiac death [65, 66]. Alterations in cardiac sympathetic function occur early in the development of heart failure. Norepinephrine release from cardiac sympathetic nerves is increased and cardiac norepinephrine reuptake is decreased, which lead to elevated cardiac sympathetic tone. Currently,

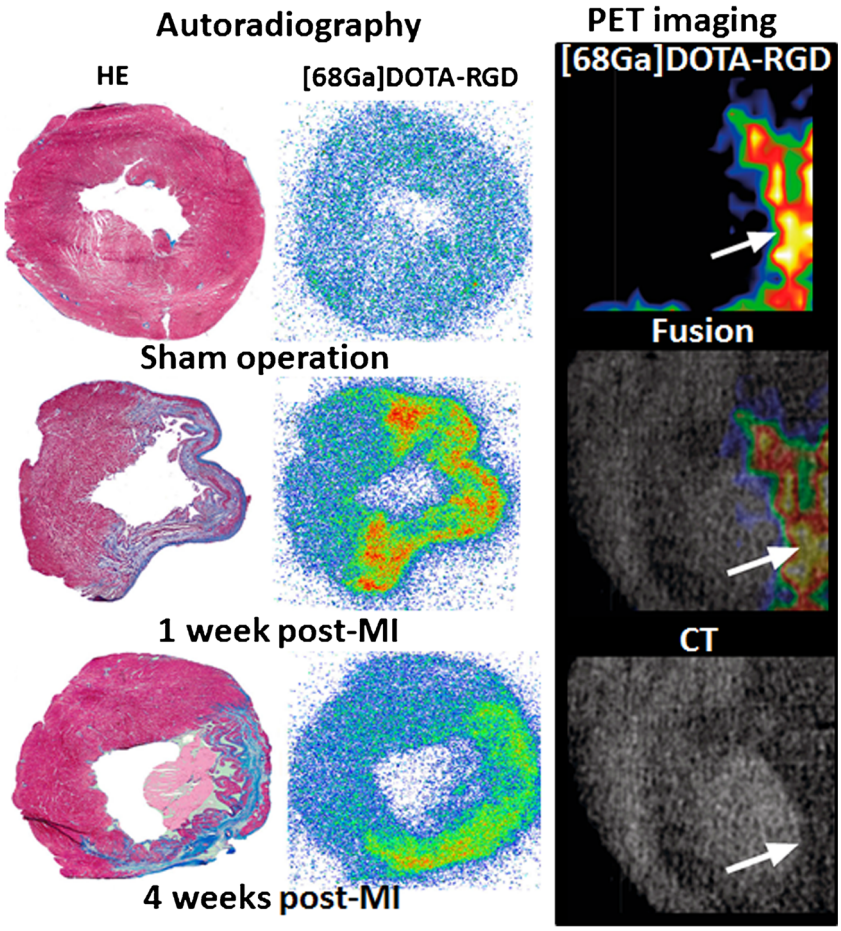

Fig. 2 Images of myocardial $\alpha_v\beta_3$ integrin upregulation evaluated by ^{68}Ga-DOTA-RGD PET after experimental myocardial infarction (MI) in rat. Autoradiographs of cross sections of the left ventricle show increased tracer uptake (*green and red color*) in the infarcted myocardium peaking at 1 week post-MI persisting at 4 weeks post-MI. Infarction is visible in the corresponding section stained with hematoxylin and eosin (HE). Micro-PET-CT images show increased tracer uptake in the anterolateral wall of the left ventricle (*arrow*) 1 week after infarction. Image adapted with permission from ref. 50

^{123}I-metaiodobenzylguanidine (^{123}I-MIBG), an iodinated neurotransmitter analog, is commonly used for SPECT imaging of sympathetic function of the heart [66]. The neuronal uptake of ^{123}I-MIBG in the heart is primarily by the norepinephrine transporter (NET), via an energy-dependent uptake 1 mechanism. Many studies have demonstrated that cardiac uptake of ^{123}I-MIBG is lower in individuals with heart failure and indicate that ^{123}I-MIBG can be used as an independent predictor of heart failure progression and cardiac mortality [66–68]. However, widespread application of ^{123}I-MIBG imaging has been limited in part by suboptimal target-to-background activity and reliance on planar imaging for quantitation of myocardial activity relative to background mediastinal activity (heart-to-mediastinum ratio) or myocardial washout. Quantification of absolute regional or global myocardial uptake has been limited.

^{11}C-metahydroxyephedrine (^{11}C-HED) is a NET ligand that has been used for PET imaging of cardiac sympathetic function. In the Prediction of ARrhythmic Events with Positron Emission Tomography (PAREPET) trial, the extent of denervation assessed with quantitative ^{11}C-HED PET was predictor of sudden cardiac arrest (arrhythmic death or intracardiac defibrillator shock for ventricular tachycardia >240/min or ventricular fibrillation) independently of ejection fraction, infarct volume, symptoms, and natriuretic peptide level in coronary artery disease patients who were candidates for an implantable cardiovertor defibrillator placement for primary prevention of sudden cardiac death [69]. A method for identifying heart failure patients with higher ejection fraction who are at hidden increased risk for lethal arrhythmias would be extremely useful as the vast majority of arrhythmic sudden cardiac death victims have minimal to no evidence specific to arrhythmic risk, but the absolute number of these patients is high [65, 66, 69]. However, widespread clinical imaging with ^{11}C-HED has been limited by the short radioactive half-life (20 min) and the need for an on-site cyclotron.

N-[3-bromo-4-(3-^{18}F-fluoro-propoxy)-benzyl]-guanidine (LMI1195) is a novel PET tracer developed for evaluation of sympathetic neuronal function in the heart [70]. This agent is a benzylguanidine analog, in the same class as MIBG, but labeled with ^{18}F, a positron emitter having half-life of 120 min. The uptake of ^{18}F-LMI1195 is NET-mediated in both rabbits and nonhuman primates and was decreased in rodent models of HF [7, 70, 71]. Experimental PET imaging studies with ^{18}F-LMI1195 showed a favorable heart-to-liver ratio, compared with ^{123}I-MIBG [70]. The initial first-in-human results of a

multicenter single-dose phase I trial indicate that clinical imaging with ^{18}F-LMI1195 is feasible for the assessment of regional myocardial sympathetic activity [72]. ^{18}F-LMI1195 was well-tolerated and yielded a radiation dose comparable to that of other commonly used PET radiopharmaceuticals. Myocardial uptake and adjacent organ activity suggest that good images should be possible with acceptable patient radiation dose. ^{18}F-LMI1195 PET imaging provides a potentially quantitative approach for evaluation of both regional denervation and the heterogeneity of innervation, indices that may be predictive of sudden cardiac death. The tracer may offer advantages over evaluation of heart-to-mediastinal ratios in future studies of patients with heart disease.

Inflammatory cardiomyopathy and cardiac sarcoidosis

It has been estimated that approximately 5% of patients with sarcoidosis will have clinically manifest cardiac involvement presenting with one or more of ventricular arrhythmias, conduction abnormalities, and heart failure. Furthermore, another 20–25% of pulmonary/systemic sarcoidosis patients have asymptomatic cardiac involvement [73]. There has been a marked increase in the detection rate of cardiac sarcoidosis that is very likely due to improved diagnostic methods and their increased use [73, 74]. The diagnosis of cardiac sarcoidosis is confirmed when non-caseating granulomas are identified in cardiac or extracardiac tissue biopsies combined with clinical manifestations and/or findings on cardiac imaging indicative of myocardial involvement [73]. The sensitivity of endomyocardial biopsy is low due to focal nature of lesions in cardiac sarcoidosis [73, 74], but may be improved if sampling is targeted with the help of cardiac imaging [75].

PET imaging for the diagnosis and monitoring of cardiac involvement in sarcoidosis has been investigated and advanced significantly in recent years. Active inflammation in cardiac sarcoidosis is detected as patchy uptake of ^{18}F-FDG that accumulates in inflammatory cells with high glucose uptake (Fig. 3). In a meta-analysis of seven diagnostic studies (164 patients with a prevalence of 50%), ^{18}F-FDG PET had a sensitivity of 89% and a specificity of 78% for cardiac sarcoidosis [77]. The findings of cardiac PET have also prognostic implications in patients with suspected cardiac sarcoidosis. In a series of 118 patients with known or suspected cardiac sarcoidosis who underwent ^{82}Rb perfusion and ^{18}F-FDG PET

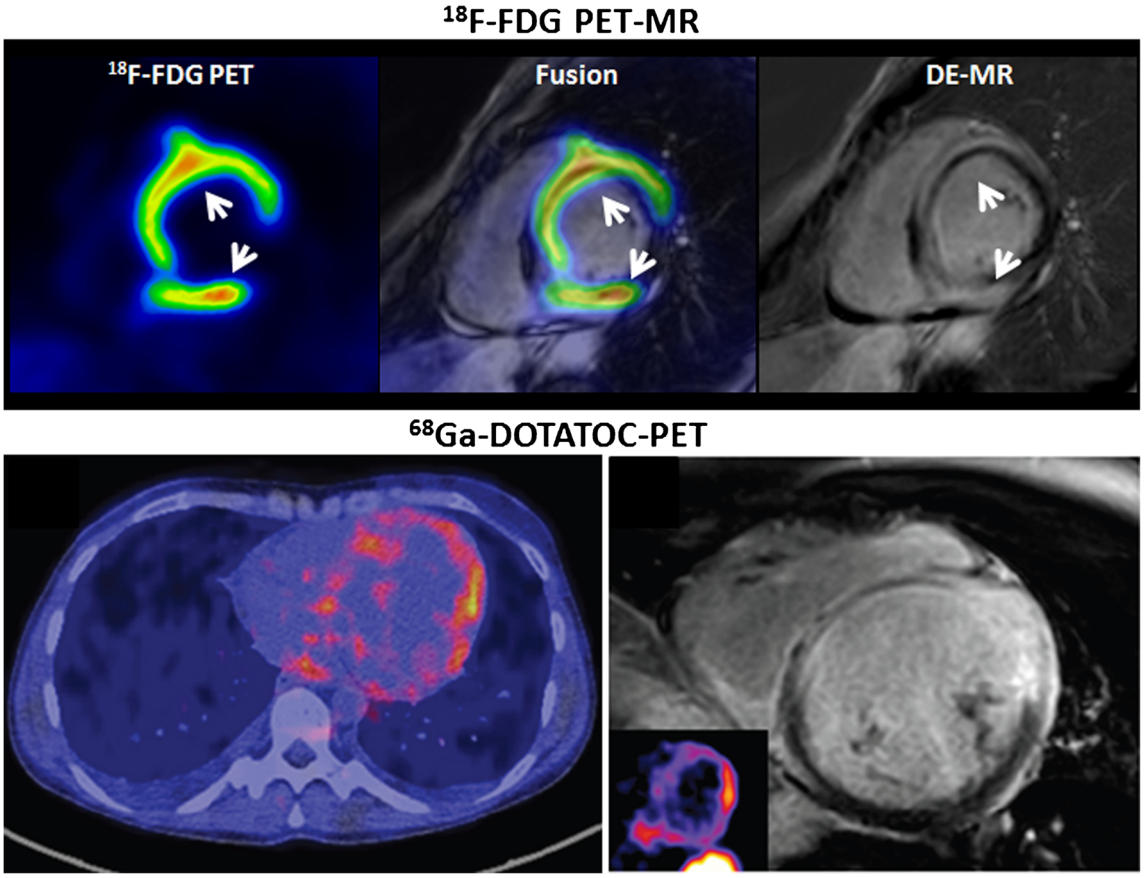

Fig. 3 Imaging of myocardial inflammation in cardiac sarcoidosis with combined ^{18}F-FDG PET (*top*) or ^{68}Ga-DOTATOC PET (*bottom*) and delayed-enhancement magnetic resonance (DE-MR). Uptake of PET tracers reflecting inflammatory activity co-localizes with myocardial injury detected with DE-MR (*arrows*). ^{68}Ga-DOTATOC PET image adapted with permission from ref. 76

imaging, abnormal perfusion and ^{18}F-FDG uptake on PET imaging predicted 2.9-times increased risk of ventricular tachycardia and death compared with normal PET results during follow-up [78]. CMR and PET are both valuable in evaluation of sarcoidosis, because they show different aspects of the disease and the relative frequency of positive findings may vary depending on clinical presentation [79]. CMR provides high resolution for identifying the presence and extent of myocardial scar, whereas ^{18}F-FDG PET is a sensitive marker of inflammatory disease activity and whole body distribution.

PET imaging for cardiac sarcoidosis requires patient preparation to suppress physiological myocardial glucose uptake since both normal myocytes and inflammatory cells take up glucose, and hence, ^{18}F-FDG. Protocols to suppress physiological myocyte ^{18}F-FDG uptake vary among studies, including prolonged fasting (12 h), high-fat and low-carbohydrate meals, and/or intravenous heparin [80]. The success of these strategies is also variable, and incomplete suppression of physiological myocardial ^{18}F-FDG uptake may significantly impair diagnostic accuracy of PET [80]. Therefore, new tracers are sought to improve specificity of PET imaging for cardiac sarcoidosis [76, 81–83].

Normal macrophages and lymphocytes have somatostatin receptors that are overexpressed in granulomatous conditions such as sarcoidosis. In exploratory studies in patients with suspected cardiac sarcoidosis, somatostatin receptor targeted PET imaging with ^{68}Ga-DOTANOC or ^{68}Ga-DOTATOC has shown promising results in the detection of active cardiac lesions as compared with ^{18}F-FDG PET or CMR (Fig. 3) [76, 81]. Since the myocardium does not display any physiologic somatostatin analogue uptake, tracer retention in the heart may be more specific than that of ^{18}F-FDG. However, the value of new tracers for the detection and monitoring treatment response in cardiac sarcoidosis remains to be tested in larger prospective studies.

Conclusions and future directions

New tracers have potential to improve availability of PET myocardial perfusion imaging that is an established tool for evaluation of ischemic etiology and the extent of viable ischemic myocardium before revascularization in heart failure. Tracers targeting $\alpha_v\beta_3$ integrin, fibrosis, or inflammatory mediators may provide biomarkers to assess functional outcome and effect of therapies on tissue repair after myocardial infarction. Innervation imaging has been shown to predict heart failure progression and risk of lethal arrhythmias. New PET tracers may facilitate adoption of quantitative measures of global and regional sympathetic nerve function. There is a need for new and more specific tracers for the diagnosis of inflammatory cardiomyopathies and cardiac sarcoidosis, which is currently a diagnostic challenge. In addition to the assessment of prognosis and etiology, the value of new PET tracers will depend on studies demonstrating their ability to guide selection of therapies and incorporation into clinical management algorithms in heart failure.

Compliance with ethical standards The authors (AS and JK) acknowledge financial support from The Academy of Finland Centre of Excellence on Cardiovascular and Metabolic Diseases, Helsinki, Finland, and Finnish Foundation for Cardiovascular Research. This article does not contain any studies with human participants or animals performed by any of the authors.

References

1. Ponikowski P, Voors AA, Anker SD et al (2016) ESC guidelines for the diagnosis and treatment of acute and chronic heart failure: the task force for the diagnosis and treatment of acute and chronic heart failure of the European Society of Cardiology (ESC). Eur Heart J 37:2129–2200
2. Bax JJ, Delgado V (2015) Myocardial viability as integral part of the diagnostic and therapeutic approach to ischemic heart failure. J Nucl Cardiol 22:229–245
3. Ylä-Herttuala S, Bridges C, Katz MG, Korpisalo P (2017) Angiogenic gene therapy in cardiovascular diseases: dream or vision? Eur Heart J 10. doi:10.1093/eurheartj/ehw547
4. Moody JB, Lee BC, Corbett JR, Ficaro EP, Murthy VL (2015) Precision and accuracy of clinical quantification of myocardial blood flow by dynamic PET: a technical perspective. J Nucl Cardiol 22:935–951
5. Bengel FM, Higuchi T, Javadi MS, Lautamäki R (2009) Cardiac positron emission tomography. J Am Coll Cardiol 54:1–15
6. Yu M, Guaraldi MT, Mistry M, Kagan M, McDonald JL, Drew K, Radeke H, Azure M, Purohit A, Casebier DS, Robinson SP (2007) BMS-747158-02: a novel PET myocardial perfusion imaging agent. J Nucl Cardiol 14:789–798
7. Jenkins WS, Vesey AT, Stirrat C, Connell M, Lucatelli C, Neale A, Moles C, Vickers A, Fletcher A, Pawade T, Wilson I, Rudd JH, van Beek EJ, Mirsadraee S, Dweck MR, Newby DE (2016) Cardiac αVβ3 integrin expression following acute myocardial infarction in humans. Heart Dec 7. doi:10.1136/heartjnl-2016-310115
8. Higuchi T, Yousefi BH, Reder S, Beschorner M, Laitinen I, Yu M, Robinson S, Wester HJ, Schwaiger M, Nekolla SG (2015) Myocardial kinetics of a novel [(18)F]-labeled sympathetic nerve PET tracer LMI1195 in the isolated perfused rabbit heart. JACC Cardiovasc Imaging 8:1229–1231
9. Teräs M, Kokki T, Durand-Schaefer N, Noponen T, Pietilä M, Kiss J, Hoppela E, Sipilä HT, Knuuti J (2010) Dual-gated cardiac PET-clinical feasibility study. Eur J Nucl Med Mol Imaging 37:505–516
10. Gaemperli O, Saraste A, Knuuti J (2012) Cardiac hybrid imaging. Eur Heart J Cardiovasc Imaging 13:51–60
11. Gheorghiade M, Sopko G, De LL, Velazquez EJ, Parker JD, Binkley PF et al (2006) Navigating the crossroads of coronary artery disease and heart failure. Circulation 114:1202–1213
12. Mc Ardle BA, Dowsley TF, deKemp RA, Wells GA, Beanlands RS (2012) Does rubidium-82 pet have superior accuracy to spect perfusion imaging for the diagnosis of obstructive coronary disease?: a systematic review and meta-analysis. J Am Coll Cardiol 60:1828–1837
13. Jaarsma C, Leiner T, Bekkers SC, Crijns HJ, Wildberger JE, Nagel E, Nelemans PJ, Schalla S (2012) Diagnostic performance of noninvasive myocardial perfusion imaging using single-photon emission computed tomography, cardiac magnetic resonance, and

positron emission tomography imaging for the detection of obstructive coronary artery disease: a meta-analysis. J Am Coll Cardiol 59: 1719–1728
14. Dorbala S, Di Carli MF, Beanlands RS, Merhige ME, Williams BA, Veledar E, Chow BJ, Min JK, Pencina MJ, Berman DS, Shaw LJ (2013) Prognostic value of stress myocardial perfusion positron emission tomography: results from a multicenter observational registry. J Am Coll Cardiol 61:176–184
15. Saraste A, Kajander S, Han C, Nesterov SV, Knuuti J (2012) PET: is myocardial flow quantification a clinical reality? J Nucl Cardiol 19:1044–1059
16. Schindler TH, Schelbert HR, Quercioli A, Dilsizian V (2010) Cardiac PET imaging for the detection and monitoring of coronary artery disease and microvascular health. JACC Cardiovasc Imaging 3:623–640
17. Johnson NP, Gould KL, Di Carli MF, Taqueti VR (2016) Invasive FFR and noninvasive CFR in the evaluation of ischemia: what is the future? J Am Coll Cardiol 67:2772–2788
18. Herzog BA, Husmann L, Valenta I, Gaemperli O, Siegrist PT, Tay FM, Burkhard N, Wyss CA, Kaufmann PA (2009) Longterm prognostic value of 13N-ammonia myocardial perfusion positron emission tomography added value of coronary flow reserve. J Am Coll Cardiol 54:150–156
19. Ziadi MC, deKemp RA, Williams KA, Guo A, Chow BJ, Renaud JM, Ruddy TD, Sarveswaran N, Tee RE, Beanlands RS (2011) Impaired myocardial flow reserve on rubidium-82 positron emission tomography imaging predicts adverse outcomes in patients assessed for myocardial ischemia. J Am Coll Cardiol 58:740–748
20. Murthy VL, Naya M, Foster CR, Hainer J, Gaber M, Di CG, Blankstein R, Dorbala S, Sitek A, Pencina MJ, Di Carli MF (2011) Improved cardiac risk assessment with noninvasive measures of coronary flow reserve. Circulation 124:2215–2224
21. Taqueti VR, Hachamovitch R, Murthy VL, Naya M, Foster CR, Hainer J, Dorbala S, Blankstein R, Di Carli MF (2015) Global coronary flow reserve is associated with adverse cardiovascular events independently of luminal angiographic severity and modifies the effect of early revascularization. Circulation 131:19–27
22. Neglia D, Michelassi C, Trivieri MG, Sambuceti G, Giorgetti A, Pratali L et al (2002) Prognostic role of myocardial blood flow impairment in idiopathic left ventricular dysfunction. Circulation 105:186–193
23. Majmudar MD, Murthy VL, Shah RV, Kolli S, Mousavi N, Foster CR, Hainer J, Blankstein R, Dorbala S, Sitek A, Stevenson LW, Mehra MR, Di Carli MF (2015) Quantification of coronary flow reserve in patients with ischaemic and non-ischaemic cardiomyopathy and its association with clinical outcomes. Eur Heart J Cardiovasc Imaging 16:900–909
24. Maddahi J, Packard RR (2014) Cardiac PET perfusion tracers: current status and future directions. Semin Nucl Med 44:333–343
25. Huisman MC, Higuchi T, Reder S, Nekolla SG, Poethko T, Wester HJ, Ziegler SI, Casebier DS, Robinson SP, Schwaiger M (2008) Initial characterization of an 18F-labeled myocardial perfusion tracer. J Nucl Med 49:630–636
26. Yu M, Guaraldi M, Kagan M, Mistry M, McDonald J, Bozek J, Yalamanchili P, Hayes M, Azure M, Purohit A, Radeke H, Casebier DS, Robinson SP (2009) Assessment of 18F-labeled mitochondrial complex I inhibitors as PET myocardial perfusion imaging agents in rats, rabbits, and primates. Eur J Nucl Med Mol Imaging 36:63–72
27. Sherif HM, Saraste A, Weidl E, Weber AW, Higuchi T, Reder S, Poethko T, Henriksen G, Casebier D, Robinson S, Wester HJ, Nekolla SG, Schwaiger M (2009) Evaluation of a novel (18)F-labeled positron-emission tomography perfusion tracer for the assessment of myocardial infarct size in rats. Circ Cardiovasc Imaging 2: 77–84
28. Maddahi J, Czernin J, Lazewatsky J, Huang SC, Dahlbom M, Schelbert H, Sparks R, Ehlgen A, Crane P, Zhu Q, Devine M, Phelps M (2011) Phase I, first-in-human study of BMS747158, a novel 18F-labeled tracer for myocardial perfusion PET: dosimetry, biodistribution, safety, and imaging characteristics after a single injection at rest. J Nucl Med 52:1490–1498
29. Berman DS, Maddahi J, Tamarappoo BK, Czernin J, Taillefer R, Udelson JE, Gibson CM, Devine M, Lazewatsky J, Bhat G, Washburn D (2013) Phase II safety and clinical comparison with single-photon emission computed tomography myocardial perfusion imaging for detection of coronary artery disease: flurpiridaz F 18 positron emission tomography. J Am Coll Cardiol 61:469–477
30. Nekolla SG, Reder S, Saraste A, Higuchi T, Dzewas G, Preissel A, Huisman M, Poethko T, Schuster T, Yu M, Robinson S, Casebier D, Henke J, Wester HJ, Schwaiger M (2009) Evaluation of the novel myocardial perfusion positron-emission tomography tracer 18F-BMS-747158-02: comparison to 13N-ammonia and validation with microspheres in a pig model. Circulation 119:2333–2342
31. Packard RR, Huang SC, Dahlbom M, Czernin J, Maddahi J (2014) Absolute quantitation of myocardial blood flow in human subjects with or without myocardial ischemia using dynamic flurpiridaz F 18 PET. J Nucl Med 55:1438–1444
32. Schinkel AF, Bax JJ, Poldermans D, Elhendy A, Ferrari R, Rahimtoola SH (2007) Hibernating myocardium: diagnosis and patient outcomes. Curr Probl Cardiol 32:375–410
33. Allman KC, Shaw LJ, Hachamovitch R, Udelson JE (2002) Myocardial viability testing and impact of revascularization on prognosis in patients with coronary artery disease and left ventricular dysfunction: a meta-analysis. J Am Coll Cardiol 39:1151–1158
34. Beanlands RS, Nichol G, Huszti E, Humen D, Racine N, Freeman M, Gulenchyn KY, Garrard L, Dekemp R, Guo A, Ruddy TD, Benard F, Lamy A, Iwanochko RM (2007) F-18-Fluorodeoxyglucose positron emission tomography imaging-assisted management of patients with severe left ventricular dysfunction and suspected coronary disease a randomized, controlled trial (PARR-2). J Am Coll Cardiol 50:2002–2012
35. Mc Ardle B, Shukla T, Nichol G, deKemp RA, Bernick J, Guo A et al. (2016) Long-term follow-up of outcomes with f-18-fluorodeoxyglucose positron emission tomography imaging-assisted management of patients with severe left ventricular dysfunction secondary to coronary disease. Circ Cardiovasc Imaging 9: e004331
36. Mielniczuk LM, Beanlands RS (2012) Does imaging-guided selection of patients with ischemic heart failure for high risk revascularization improve identification of those with the highest clinical benefit? Imaging-guided selection of patients with ischemic heart failure for high-risk revascularization improves identification of those with the highest clinical benefit. Circ Cardiovasc Imaging 5:262–270
37. Ling LF, Marwick TH, Flores DR, Jaber WA, Brunken RC, Cerqueira MD, Hachamovitch R (2013) Identification of therapeutic benefit from revascularization in patients with left ventricular systolic dysfunction: inducible ischemia versus hibernating myocardium. Circ Cardiovasc Imaging 6:363–372
38. Bonow RO, Maurer G, Lee KL, Holly TA, Binkley PF, Desvigne-Nickens P et al (2011) Myocardial viability and survival in ischemic left ventricular dysfunction. N Engl J Med 364:1617–1625
39. Knaapen P, Germans T, Knuuti J, Paulus WJ, Dijkmans PA, Allaart CP, Lammertsma AA, Visser FC (2007) Myocardial energetics and efficiency: current status of the noninvasive approach. Circulation 115:918–927
40. Tuunanen H, Knuuti J (2011) Metabolic remodelling in human heart failure. Cardiovasc Res 90:251–257
41. Sutton MG, Sharpe N (2000) Left ventricular remodeling after myocardial infarction: pathophysiology and therapy. Circulation 101:2981–2988

42. de Haas HJ, Arbustini E, Fuster V, Kramer CM, Narula J (2014) Molecular imaging of the cardiac extracellular matrix. Circ Res 114:903–915
43. Hulsmans M, Sam F, Nahrendorf M (2016) Monocyte and macrophage contributions to cardiac remodeling. J Mol Cell Cardiol 93: 149–155
44. Meoli DF, Sadeghi MM, Krassilnikova S, Bourke BN, Giordano FJ, Dione DP, Su H, Edwards DS, Liu S, Harris TD, Madri JA, Zaret BL, Sinusas AJ (2004) Noninvasive imaging of myocardial angiogenesis following experimental myocardial infarction. J Clin Invest 113:1684–1691
45. Sun M, Opavsky MA, Stewart DJ, Rabinovitch M, Dawood F, Wen WH, Liu PP (2003) Temporal response and localization of integrins beta1 and beta3 in the heart after myocardial infarction: regulation by cytokines. Circulation 107:1046–1052
46. Van den Borne SWM, Isobe S, Verjans JW, Petrov A, Lovhaug D, Li P et al (2008) Molecular imaging of interstitial alterations in remodeling myocardium after myocardial infarction. J Am Coll Cardiol 52:2017–2028
47. Higuchi T, Bengel FM, Seidl S, Watzlowik P, Kessler H, Hegenloh R, Reder S, Nekolla SG, Wester HJ, Schwaiger M (2008) Assessment of alphavbeta3 integrin expression after myocardial infarction by positron emission tomography. Cardiovasc Res 78: 395–403
48. Sherif HM, Saraste A, Nekolla SG, Weidl E, Reder S, Tapfer A, Rudelius M, Higuchi T, Botnar RM, Wester H-J, Schwaiger M (2012) Molecular imaging of early αvβ3 integrin expression predicts long-term left-ventricle remodeling after myocardial infarction in rats. J Nucl Med 53:318–323
49. Gao H, Lang L, Guo N, Cao F, Quan Q, Hu S, Kiesewetter DO, Niu G, Chen X (2012) PET imaging of angiogenesis after myocardial infarction/reperfusion using a one-step labeled integrin-targeted tracer 18F-AlF-NOTA-PRGD2. Eur J Nucl Med Mol Imaging 39: 683–692
50. Kiugel M, Dijkgraaf I, Kytö V, Helin S, Liljenbäck H, Saanijoki T, Yim C-B, Oikonen V, Saukko P, Knuuti J, Roivainen A, Saraste A (2014) Dimeric [(68)Ga]DOTA-RGD peptide targeting αvβ 3 integrin reveals extracellular matrix alterations after myocardial infarction. Mol Imaging Biol 16:793–801
51. Knetsch PA, Petrik M, Griessinger CM, Rangger C, Fani M, Kesenheimer C, von Guggenberg E, Pichler BJ, Virgolini I, Decristoforo C, Haubner R (2011) [68Ga]NODAGA-RGD for imaging αvβ3 integrin expression. Eur J Nucl Med Mol Imaging 38: 1303–1312
52. Laitinen I, Notni J, Pohle K, Rudelius M, Farrell E, Nekolla SG, Henriksen G, Neubauer S, Kessler H, Wester H-J, Schwaiger M (2013) Comparison of cyclic RGD peptides for αvβ3 integrin detection in a rat model of myocardial infarction. EJNMMI Res 3:38
53. Menichetti L, Kusmic C, Panetta D, Arosio D, Petroni D, Matteucci M, Salvadori PA, Casagrande C, L'Abbate A, Manzoni L (2013) MicroPET/CT imaging of $\alpha v\beta_3$ integrin via a novel 68Ga-NOTA-RGD peptidomimetic conjugate in rat myocardial infarction. Eur J Nucl Med Mol Imaging 40:1265–1274
54. Sun Y, Zeng Y, Zhu Y, Feng F, Xu W, Wu C, Xing B, Zhang W, Wu P, Cui L, Wang R, Li F, Chen X, Zhu Z (2014) Application of (68)Ga-PRGD2 PET/CT for αvβ3-integrin imaging of myocardial infarction and stroke. Theranostics 4:778–786
55. Prior JO, Farhad H, Muller O (2014) Multimodality imaging in ischemic cardiomyopathy. Curr Cardiovasc Imaging Rep 7:9285
56. Makowski MR, Ebersberger U, Nekolla S, Schwaiger M (2008) In vivo molecular imaging of angiogenesis, targeting alphavbeta3 integrin expression, in a patient after acute myocardial infarction. Eur Heart J 29:2201
57. Verjans J, Wolters S, Laufer W, Schellings M, Lax M, Lovhaug D, Boersma H, Kemerink G, Schalla S, Gordon P, Teule J, Narula J, Hofstra L (2010) Early molecular imaging of interstitial changes in patients after myocardial infarction: comparison with delayed contrast-enhanced magnetic resonance imaging. J Nucl Cardiol 17:1065–1072
58. Rischpler C, Dirschinger RJ, Nekolla SG, Kossmann H, Nicolosi S, Hanus F et al (2016) Prospective evaluation of 18F-fluorodeoxyglucose uptake in postischemic myocardium by simultaneous positron emission tomography/magnetic resonance imaging as a prognostic marker of functional outcome. Circ Cardiovasc Imaging 9:e004316
59. Thackeray JT, Bankstahl JP, Wang Y, Wollert KC, Bengel FM (2016) Targeting amino acid metabolism for molecular imaging of inflammation early after myocardial infarction. Theranostics 6: 1768–1779
60. Thackeray JT, Derlin T, Haghikia A, Napp LC, Wang Y, Ross TL, Schäfer A, Tillmanns J, Wester HJ, Wollert KC, Bauersachs J, Bengel FM (2015) Molecular imaging of the chemokine receptor CXCR4 after acute myocardial infarction. JACC Cardiovasc Imaging 8:1417–1426
61. Lapa C, Reiter T, Werner RA, Ertl G, Wester HJ, Buck AK, Bauer WR, Herrmann K (2015) [(68)Ga]Pentixafor-PET/CT for imaging of chemokine receptor 4 expression after myocardial infarction. JACC Cardiovasc Imaging 8:1466–1468
62. Rischpler C, Nekolla SG, Kossmann H, Dirschinger RJ, Schottelius M, Hyafil F, Wester HJ, Laugwitz KL, Schwaiger M (2016) Upregulated myocardial CXCR4-expression after myocardial infarction assessed by simultaneous GA-68 pentixafor PET/MRI. J Nucl Cardiol 23:131–133
63. Kiugel M, Kytö V, Saanijoki T, Liljenbäck H, Metsälä O, Ståhle M, Tuomela J, Li XG, Saukko P, Knuuti J, Roivainen A, Saraste A (2016) Evaluation of 68Ga-labeled peptide tracer for detection of gelatinase expression after myocardial infarction in rat. J Nucl Cardiol. doi:10.1007/s12350–016–0744-4
64. Fukushima K, Bravo PE, Higuchi T, Schuleri KH, Lin X, Abraham MR, Xia J, Mathews WB, Dannals RF, Lardo AC, Szabo Z, Bengel FM (2012) Molecular hybrid positron emission tomography/computed tomography imaging of cardiac angiotensin II type 1 receptors. J Am Coll Cardiol 60:2527–2534
65. Juneau D, Erthal F, Chow BJ, Redpath C, Ruddy TD, Knuuti J, Beanlands RS (2016) The role of nuclear cardiac imaging in risk stratification of sudden cardiac death. J Nucl Cardiol 23:1380–1398
66. Travin MI (2017) Current clinical applications and next steps for cardiac innervation imaging. Curr Cardiol Rep 19:1
67. Jacobson AF, Senior R, Cerqueira MD, Wong ND, Thomas GS, Lopez VA, Agostini D, Weiland F, Chandna H, Narula J, ADMIRE-HF Investigators (2010) Myocardial iodine-123 meta-iodobenzylguanidine imaging and cardiac events in heart failure. Results of the prospective ADMIRE-HF (AdreView myocardial imaging for risk evaluation in heart failure) study. J Am Coll Cardiol 55:2212–2221
68. Narula J, Gerson M, Thomas GS, Cerqueira MD, Jacobson AF (2015) ^{123}I-MIBG imaging for prediction of mortality and potentially fatal events in heart failure: the ADMIRE-HFX study. J Nucl Med 56:1011–1018
69. Fallavollita JA, Heavey BM, Luisi AJ Jr, Michalek SM, Baldwa S, Mashtare TL Jr, Hutson AD, Dekemp RA, Haka MS, Sajjad M, Cimato TR, Curtis AB, Cain ME, Canty JM Jr (2014) Regional myocardial sympathetic denervation predicts the risk of sudden cardiac arrest in ischemic cardiomyopathy. J Am Coll Cardiol 63: 141–149
70. Yu M, Bozek J, Lamoy M, Guaraldi M, Silva P, Kagan M, Yalamanchili P, Onthank D, Mistry M, Lazewatsky J, Broekema M, Radeke H, Purohit A, Cdebaca M, Azure M, Cesati R, Casebier D, Robinson SP (2011) Evaluation of LMI1195, a novel 18F-labeled cardiac neuronal PET imaging agent, in cells and animal models. Circ Cardiovasc Imaging 4:435–443

71. Werner RA, Rischpler C, Onthank D, Lapa C, Robinson S, Samnick S, Javadi M, Schwaiger M, Nekolla SG, Higuchi T (2015) Retention kinetics of the 18F-labeled sympathetic nerve PET tracer LMI1195: comparison with 11C-Hydroxyephedrine and 123I-MIBG. J Nucl Med 56:1429–1433
72. Sinusas AJ, Lazewatsky J, Brunetti J, Heller G, Srivastava A, Liu YH, Sparks R, Puretskiy A, Lin SF, Crane P, Carson RE, Lee LV (2014) Biodistribution and radiation dosimetry of LMI1195: first-in-human study of a novel 18F-labeled tracer for imaging myocardial innervation. J Nucl Med 55:1445–1451
73. Birnie DH, Kandolin R, Nery PB, Kupari M (2016) Cardiac manifestations of sarcoidosis: diagnosis and management. Eur Heart J. doi:10.1093/eurheartj/ehw328
74. Youssef G, Beanlands RS, Birnie DH et al (2011) Cardiac sarcoidosis: applications of imaging in diagnosis and directing treatment. Heart 97:2078–2087
75. Simonen P, Lehtonen J, Kandolin R et al (2015) 18F-fluorodeoxyglucose positron emission tomography-guided sampling of mediastinal lymph nodes in the diagnosis of cardiac sarcoidosis. Am J Cardiol 116:1581–1585
76. Lapa C, Reiter T, Kircher M, Schirbel A, Werner RA, Pelzer T, Pizarro C, Skowasch D, Thomas L, Schlesinger-Irsch U, Thomas D, Bundschuh RA, Bauer WR, Gärtner FC (2016) Somatostatin receptor based PET/CT in patients with the suspicion of cardiac sarcoidosis: an initial comparison to cardiac MRI. Oncotarget 7:77807–77814
77. Youssef G, Leung E, Mylonas I et al (2012) The use of 18F-FDG PET in the diagnosis of cardiac sarcoidosis: a systematic review and metaanalysis including the Ontario experience. J Nucl Med 53:241–248
78. Blankstein R, Osborne M, Naya M, Waller A, Kim CK, Murthy VL et al (2014) Cardiac positron emission tomography enhances prognostic assessments of patients with suspected cardiac sarcoidosis. J Am Coll Cardiol 63:329–336
79. Ohira H, Birnie DH, Pena E, Bernick J, Mc Ardle B, Leung E et al (2016) Comparison of (18)F-fluorodeoxyglucose positron emission tomography (FDG PET) and cardiac magnetic resonance (CMR) in corticosteroid-naive patients with conduction system disease due to cardiac sarcoidosis. Eur J Nucl Med Mol Imaging 43:259–269
80. Tang R, Wang JT, Wang L, Le K, Huang Y, Hickey AJ, Emmett L (2016) Impact of patient preparation on the diagnostic performance of 18F-FDG PET in cardiac sarcoidosis: a systematic review and meta-analysis. Clin Nucl Med 41:e327–e339
81. Gormsen LC, Haraldsen A, Kramer S, Dias AH, Kim WY, Borghammer P (2016) A dual tracer (68)Ga-DOTANOC PET/CT and (18)F-FDG PET/CT pilot study for detection of cardiac sarcoidosis. EJNMMI Res 6:52
82. Chae SY, Choi CM, Shim TS, Park Y, Park CS, Lee HS, Lee SJ, Oh SJ, Kim SY, Baek S, Koglin N, Stephens AW, Dinkelborg LM, Moon DH (2016) Exploratory clinical investigation of (4S)-4-(3-18F-Fluoropropyl)-L-glutamate PET of inflammatory and infectious lesions. J Nucl Med 57:67–69
83. Norikane T, Yamamoto Y, Maeda Y, Noma T, Nishiyama Y (2015) 18F-FLT PET imaging in a patient with sarcoidosis with cardiac involvement. Clin Nucl Med 40:433–434